Available online at www.sciencedirect.com
ScienceDirect
Bioorganic & Medicinal Chemistry 16 (2008) 2665–2675
Bioorganic & Medicinal Chemistry

Structural insights into hydroxycoumarin-induced apoptosis in U-937 cells

Maria E. Riveiro,[a,d,e] Albertina Moglioni,[b,e] Ramiro Vazquez,[a,d,e] Natalia Gomez,[b,e] Graciela Facorro,[c] Lidia Piehl,[c] Emilio Rubin de Celis,[c] Carina Shayo[d,e] and Carlos Davio[a,e,*]

[a]*Laboratorio de Radioisótopos, Facultad de Farmacia y Bioquímica, Argentina*
[b]*Cátedra de Química Medicinal, Facultad de Farmacia y Bioquímica, Argentina*
[c]*Cátedra de Física, Facultad de Farmacia y Bioquímica, Universidad de Buenos Aires, Argentina*
[d]*Laboratorio de Patología Molecular, Instituto de Biología y Medicina Experimental, Buenos Aires, Argentina*
[e]*Consejo Nacional de Investigaciones Científicas y Técnicas, Buenos Aires, Argentina*

Received 4 October 2007; revised 10 November 2007; accepted 13 November 2007
Available online 19 November 2007

Abstract—In the present study, we sought to establish the effect of diverse structural-related hydroxycoumarins on the proliferation, cytotoxicity, and induction of apoptosis in promonocytic leukemic cells (U-937). The dihydroxylated coumarins, 7,8-dihydroxy-coumarin and esculetin, induced DNA fragmentation as well as characteristic morphological changes of programmed cell death in U-937 cells. With the aim to perform a structure-activity relationship study, the correlation between the physicochemical properties of the molecules and their pro-apoptotic activity was carried out. Results showed that the presence of two adjacent phenolic hydroxyl groups was the most important factor in terms of the SAR. The exposure of leukemic cells to 7,8-dihydroxy-coumarin evoked a phenoxyl radical generation that was detected by electron spin resonance spectroscopy. The present study suggests that reactive oxygen species generation plays a critical role in dihydroxycoumarin-induced apoptosis in U-937 cells. These findings further suggest that these compounds may have a potential therapeutic role in the treatment of hematological malignancies.

1. Introduction

Acute leukemia is a malignant neoplasm of the hematopoietic cells characterized by an abnormal proliferation of precursor cells, decreased rate of apoptosis, and arrest in cell differentiation.[1] This makes induction of apoptosis in leukemic cells a valuable therapeutic tool. Unfortunately many leukemias turn refractory to chemotherapy strongly supporting the necessity of alternative chemotherapeutic strategies.[1] Nowadays, many of the therapeutic agents used in the treatment of malignant neoplasm including VP16, cisplatin, adriamycin, and taxol exert their anti-cancer effects by inducing apoptosis of cancer cells.[2,3]

Great efforts have been made in the past years in the search of new compounds for the treatment of leukemias. Based on their low toxicity, relative low cost, and their presence in the diet and herbal medicines, it is highly interesting to examine the pharmacological behavior and eventual future applications of coumarins. In previous studies we reported that a group of natural coumarins shows anti-proliferative and differentiation activity in the promonocytic U-937 cell line.[4] Recently, we described that the 7,8-dihydroxy-4-methylcoumarin induces selective apoptosis in U-937 and HL-60 leukemic cells mediated by the activation or inhibition of the major signaling pathways as the mitogen-activated protein kinases (MAPKs), phosphoinositide-3-kinase/Akt signaling cascade (PI3K/Akt), c-myc proto-oncogene, and caspase-3.[5] In order to gain insight into the pharmacological properties of the hydroxycoumarins, we performed a study to understand the relationship between the structure and the biological activity.

Natural as well as synthetic coumarins have recently drawn much attention due to its broad pharmacological

Keywords: Hydroxycoumarins; Free radicals; Apoptosis induction; Leukemia.
* Corresponding author. Tel.: +54 114964 8277x35; fax: +54 114786 2564; e-mail: cardavio@ffyb.uba.ar

0968-0896/$ - see front matter © 2007 Elsevier Ltd. All rights reserved.
doi:10.1016/j.bmc.2007.11.038

activities.[6–8] Many coumarins and their derivatives exert in vitro and in vivo scavenging of reactive oxygen species (ROS), anti-coagulant,[9] anti-inflammatory,[10] and anti-viral effects.[11] In sensitive neoplasms, coumarins and derivatives cause significant changes in cell growth and differentiation.[4,5] Furthermore, coumarin derivatives modulate multidrug resistance transporters which are intimately related with the resistance developed to diverse chemotherapeutic therapies.[12] Recent studies showed that coumarins display antimicrobial activity depending on their structure. The presence of a free 6-OH on the coumarin nucleus is correlated with antifungal activity, whereas a free 7-OH with antibacterial activity. Moreover, a structure-activity relationship study of coumarins acting on xanthine oxidase reveals that at least one hydroxyl group is required for such activity.[6]

Furthermore, hydroxycoumarins with an aromatic nitro group display anti-proliferative and pro-apoptotic effects in renal carcinoma and leukemic cells.[13,14] In addition, the most cytotoxic compound in lung carcinoma and colon adenocarcinoma cell lines has at least two polar functional groups on the aromatic ring of the coumarinic nucleus.[15] The hydroxylated coumarins, esculetin and scopoletin, exhibit anti-tumoral effects by inducing programmed cell death in HL-60 cells.[16,17] These studies strongly support that the biological activity and therapeutic applications of hydroxycoumarins are tightly related to their structure, namely, the pattern of substitution on the aromatic ring.

Classically dietary phenols and polyphenols are considered antioxidants, but recent studies show that they also display pro-oxidant properties.[18] Some plant isolated or synthetic coumarins exhibit significant anti-oxidant activity based on their ability to inhibit lipid peroxidation and to scavenge reactive species.[10,19,11] It has been reported that dihydroxy-4-methylcoumarins favor the inhibition of lipid peroxidation by scavenging free radicals through chelation and by preventing the formation of superoxide and other ROS.[20] In a comprehensive review, Hoult and Paya[8] describe that dihydroxylated coumarins fraxetin, esculetin, 4-methylesculetin, daphnetin, and 4-methyldaphnetin, are not only effective inhibitors of Fe^{3+}-ascorbate-dependent microsomal lipid peroxidation and of aqueous alkylperoxyl radicals, but also scavengers of superoxide anion radicals. However coumarins with *ortho*-dihydroxylation enhance hydroxyl radical generation in the Fe^{3+}–EDTA–H_2O_2 deoxyribose system, but decrease it in the Fe^{3+}–ascorbate–H_2O_2 deoxyribose system, supporting that they can chelate iron ions and also donate electrons, promoting a Fenton type reaction. These findings support that hydroxylated coumarins may either behave as ROS scavengers or pro-oxidant compounds depending on factors such as metal-reducing potential, metal chelating behavior, pH as well as solubility.[21] Scopoletin induces apoptosis in HL-60 cells, but the effect is prevented by an antioxidant, suggesting that the generation of ROS may contribute to scopoletin-induced apoptosis.[17] Various reports propose that the pro-oxidant action of plant derived phenolics rather than their antioxidant action may be an important mechanism for their pro-apoptotic properties in cancer cells.[22]

The present study evaluates the key structural requirements of related hydroxycoumarins to induce apoptosis in a leukemic cell line. We provide evidence of a clear relationship between the pro-oxidant activity of hydroxycoumarins and their ability to induce apoptosis. These findings further suggest that these compounds may have a potential therapeutic role in the future.

2. Results and discussion

We have recently demonstrated that the treatment with micromolar concentrations of 7,8-dihydroxy-4-methylcoumarin (namely compound **8** in this report) induces selective apoptosis in human leukemia cells.[5] With the aim to perform a structure–activity relationship (SAR) study, the correlation between the physicochemical properties of structurally related hydroxycoumarins and their pro-apoptotic activity was evaluated.

Scheme 1 illustrates the chemical synthesis of the coumarins that were biologically assayed, whereas Table 1 lists all the compounds analyzed. The coumarin compounds (Scheme 1) were synthesized through the Pechmann reaction between a properly substituted phenol and ethyl acetoacetate. The obtained yields ranged between 20% and 80%, depending on the starting phenol used in the reaction. All the synthesized coumarins had a methyl group in C-4 of the coumarin ring due

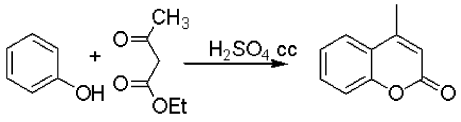

Scheme 1. General synthesis of coumarins.

Table 1. Structure of natural and synthetic coumarins

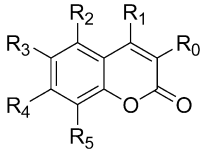

	R_0	R_1	R_2	R_3	R_4	R_5
1	–H	–H	–H	–H	–H	–H
2	–H	–H	–H	–OH	–OH	–H
3	–H	–H	–H	$–OCH_3$	–OH	–H
4	–H	$–CH_3$	–H	–H	–H	$–CH_3$
5	–H	$–CH_3$	–H	–H	$–CH_3$	–H
6	–H	$–CH_3$	–H	$–CH_3$	–H	–H
7	–H	$–CH_3$	–H	–H	–OH	–H
8	–H	$–CH_3$	–H	–H	–OH	–OH
9	–H	$–CH_3$	–H	–OH	–H	–H
10	–H	$–CH_3$	–H	–H	$–NH_2$	–H
11	–H	$–CH_3$	–H	–H	$–OCH_3$	–H
12	–H	$–CH_3$	–H	–H	–OH	–H
13	OH	–H	–H	–H	–H	–H

to the ethyl acetoacetate as β-ketoester used in the Pechmann reaction. Compounds **1**, **2**, **3**, **12**, and **13** without a methyl group in C-4 were commercial coumarins. The methylation of the 7-hydroxy group or the change of the hydroxyl group by an amine group in compound **7** was present in the commercial compounds **11** and **10**. The selection of this type of substitution led us to evaluate the influence of one or two hydroxy groups in different positions of the coumarin nucleus, as well as the effect of the alkylation of the hydroxy group, and its replacement by an amino or methyl group. The selected compounds also differed in their substitution in C-4: methyl, hydrogen or $-CF_3$, groups. Each chemical group exhibits different electronic properties which may eventually impact on the biological activity displayed by these compounds.

All coumarin analogues were tested for their potential proliferative and cytotoxic effect on U-937 cells. Cell growth, assessed by [^{3}H] thymidine incorporation, was inhibited by the two dihydroxylated coumarins (**8** and **2**) in a concentration-dependent manner. The inhibitory concentration 50 (IC_{50}) values for coumarins **8** and **2** were 48.65 ± 1.50 μM and 31.33 ± 1.20 μM, respectively (Table 2). Coumarins **2** and **8** bearing two free hydroxyl groups on the aromatic ring were more potent than coumarins **3**, **7**, and **9,** which had only one free hydroxyl aromatic group (IC_{50} values were 151.50 ± 1.04, 710.90 ± 1.26, and 627.70 ± 1.78 μM, respectively). The remainder coumarins failed to inhibit cell growth at a concentration lower than 2 mM (Table 2). Similar results were obtained with a cellular meter Coulter Z-1 (data not shown).

Table 2. Effect of coumarins on U-937 cell proliferation and cytotoxicity

Coumarins	CC_{50} (μM) Means ± SEM	IC_{50} (μM) Means ± SEM
Dihydroxycoumarins		
8	165.40 ± 1.80	48.65 ± 1.50
2	194.10 ± 2.34	31.33 ± 1.20
Monohydroxycoumarins		
7	>2000	710.90 ± 1.26
3	600.20 ± 8.54	151.50 ± 1.04
12	>2000	>2000
13	>2000	>2000
9	>2000	627.70 ± 1.78
Dimethyl coumarins		
4	>2000	>2000
5	>2000	>2000
6	>2000	> 2000
4-Methyl-7-substituted coumarins		
10	>2000	>2000
11	>2000	>2000
Coumarin	>2000	>2000

Cell growth of control and treated U-937 cells was assessed by [^{3}H] thymidine incorporation. Cellular toxicity was evaluated by the Trypan blue assay. IC_{50} and CC_{50} values were calculated with the equation for sigmoidal dose response using Prism 4.00 for Windows (GraphPad Software, San Diego, CA). Data are means ± SEM (n = 4).

The cytotoxic concentration 50 (CC_{50}) for the tested coumarins was determined by the Trypan blue dye exclusion assay. The most potent cytotoxic activity was observed for coumarins **8** and **2**, followed by compound **3** (Table 2). On the other hand, coumarins **7** and **9** as well as the other evaluated compounds did not affect cell viability at a concentration lower than 2 mM (Table 2). Incubation of U-937 cells with 0.0001% (v/v) DMSO showed that the vehicle failed to influence cell proliferation or to exhibit cytotoxicity per se.

Previously, we demonstrated that compound **8** induced programmed cell death in a concentration and time-dependent manner in U-937 cells. A ladder-like pattern of DNA fragments or morphological changes were clearly observed at concentrations higher than 250 μM.[5] A characterized key marker of cellular apoptosis is DNA cleavage into nucleosomal size fragments of 180–200 base pairs or multiples thereof, which are detected by gel electrophoresis as a DNA ladder.[23] Figure 1 shows that DNA fragmentation became evident in U-937 cells treated with 250 μM or 2 mM coumarins **8** or **2** for 24 h. Monohydroxycoumarins as **7**, **3** or **9** did not induce DNA fragmentation at 250 μM, but the ladder was observed at 2 mM. Compound **12**, a monohydroxy-

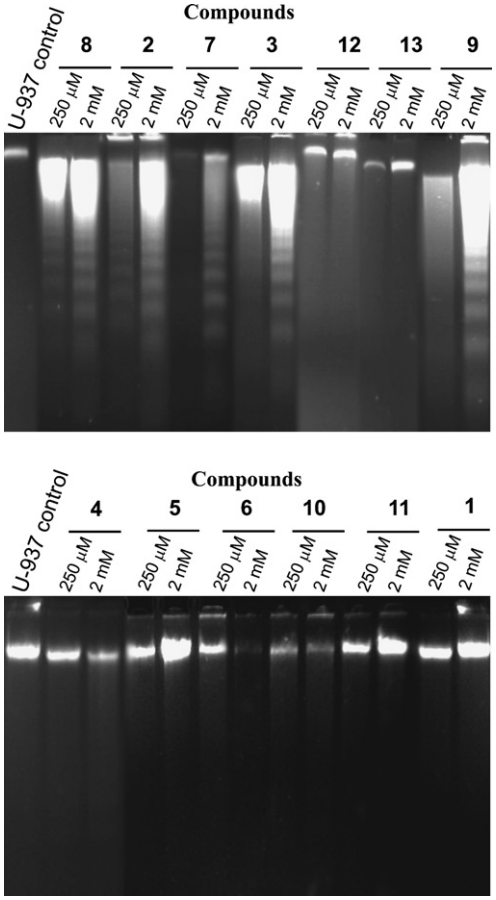

Figure 1. DNA fragmentation analysis. After the incubation of cells with 250 μM or 2 mM coumarins for 24 h the genomic DNA from treated and untreated cells was subjected to agarose gel electrophoresis. Similar results were obtained in three independent experiments.

coumarin with a strong attractor electron group like trifluoromethyl or **13** with a hydroxyl group in the pyrone ring, failed to induce apoptosis at any concentration. The other structurally related coumarins (**1**, **4**, **5**, **6**, **10**, and **11**) did not produce DNA fragmentation at 250 μM or 2 mM (Fig. 1). To further characterize programmed cell death induced by hydroxycoumarins, we examined the nuclear morphology of treated and untreated cells by the Hoechst/propidium iodide membrane permeability assay.[24] Morphological changes as condensed chromatin, fragment nuclei, and apoptotic bodies are features of the apoptotic process.[25] After 24 h of treatment with these structurally related number of apoptotic cells was estimated by the appropriate changes of nuclei stained with Hoechst 33342 observed under a fluorescence microscope. Only cells treated with 250 μM of coumarin **8** or **2** for 24 h showed a number of apoptotic cells significantly different with respect to control cells (Table 3). Figure 2A shows the morphological changes corresponding to the apoptotic process in coumarin **8** treated cells. According to this, May Grunwald–Giemsa staining of U-937 cells previously exposed to 250 μM coumarins for 48 h showed that only coumarins **8** or **2** induced chromatin condensation, nuclear segmentation, and cell shrinkage. In contrast, U-937 cells treated with compounds **7** or **1** did not exhibit these characteristic morphological alterations (Fig. 2B). Similar results were obtained in the presence of the remainder coumarins (data not shown).

We next attempted to correlate the physicochemical properties of the molecules with their in vitro activity.

Table 3. Effect of coumarins on U-937 cell apoptosis

	Percentage of apoptotic U-937 cells (means ± SEM)		Percentage of apoptotic U-937 cells (means ± SEM)
U-937 Control cells	3.3 ± 1.5	Compound **7**	5.2 ± 2.4
Compound **1**	2.6 ± 0.8	Compound **8**	55.0 ± 3.2**
Compound **2**	54.3 ± 5.4**	Compound **9**	3.0 ± 1.1
Compound **3**	6.3 ± 1.8	Compound **10**	4.0 ± 1.0
Compound **4**	4.6 ± 0.8	Compound **11**	4.0 ± 1.2
Compound **5**	5.3 ± 1.4	Compound **12**	4.7 ± 1.2
Compound **6**	4.3 ± 1.2	Compound **13**	5.3 ± 1.8

Cells were incubated with 250 μM of the assessed coumarins for 24 h.

Apoptotic cells were visualized by the appropriate changes of nuclei stained with Hoechst 33342/propidium iodide dyes and observed under a fluorescence microscope under UV light at 430 nm and 100 cells were minimally counted. Values are mean ± SEM ($n = 3$); $^{**}p < 0.01$ vs control group.

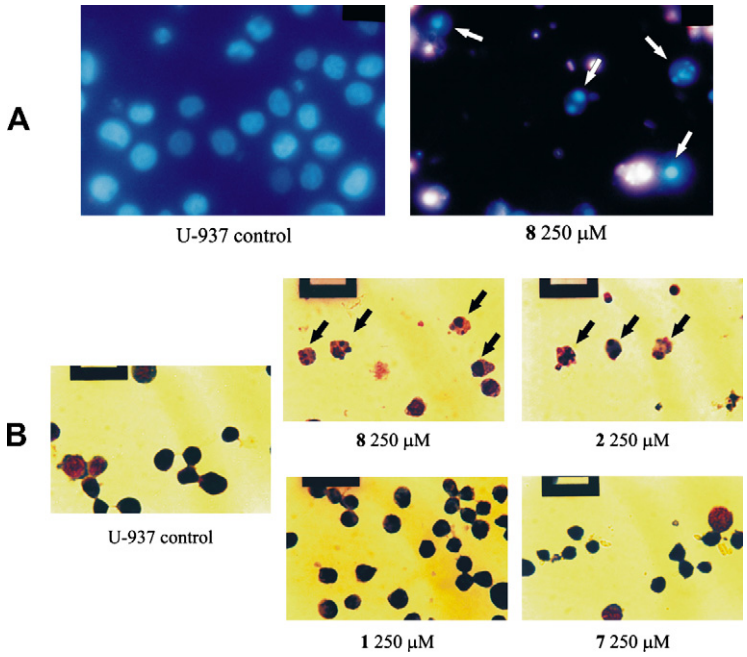

Figure 2. Morphological changes in U-937 cells associated with the apoptotic process induced by coumarins. (A) Nuclear staining with Hoechst 33342/propidium iodide dyes. U-937 cells exposed to coumarin **8** for 24 h were observed under a fluorescence microscope at 430 nm. Arrows represent condensed chromatin, fragmented nuclei, and apoptotic bodies. Each picture is representative of three independent experiments. (B) Cells were exposed to 250 μM of coumarins **8**, **2**, **7**, and **1** for 48 h. Treated and untreated U-937 cells were then stained with May Grunwald–Giemsa stain, and cell morphology determined by light microscopy. Arrows represent chromatin condensation, nuclear segmentation, and cell shrinkage. Each picture is representative of three independent experiments.

Results showed that the presence of two adjacent phenolic hydroxyl groups was the most important factor in terms of SAR, whereas the position of the *o*-dihydroxyl groups in the aromatic nucleus had little effect. Similar SAR results were previously reported for hydroxycoumarins as inducers of Cu^{2+}-dependent DNA strand breakage.[26] Moreover we found that other structural characteristic of coumarins also influenced their pro-apoptotic activity. The methylation of the 6-OH group in coumarin **3** reduced the biological activity but the loss of activity was higher in monohydroxy-derivatives, as coumarin **7** or **9**. We also observed that the derivatives where the phenolic hydroxyl group was replaced by amino or methyl groups (compounds **10** and **4**–**6**) failed to exhibit pro-apoptotic activity in U-937 cells. Furthermore, modification of the hydroxyl aromatic group by methylation (coumarin **11**) led to a loss of the biological activity. In accordance with our findings, it has been reported that coumarin derivatives are potent inhibitors of 5-hydroxy-6,8,11,14-eicosatetraenoic acid (5-HETE) formation from arachidonic acid and 12-hydroxy-5,8,10-heptadecatrienoic acid in polymorphonuclear leukocytes. The inhibitory effect is dependent on the presence of two adjacent phenolic hydroxyl groups in the coumarinic structure at positions C-6 and C-7 or C-7 and C-8. On the other hand, monohydroxycoumarins, as 7-hydroxycoumarin and scopoletin, show a weak inhibition of 5-HETE formation.[27] The presence of a methyl or hydrogen group in position 4 of the coumarin ring in most of the derivatives did not influence their pro-apoptotic activity but the presence of a $-CF_3$ group affected the biological activity of monohydroxycoumarins (coumarins **7** vs **12**), likely as the result of the different electronic properties of this group. On the other hand, the presence of a vinylic hydroxyl group in the 1,2-pyrone ring or the coumarin itself did not display pro-apoptotic activity in leukemic cells.

It is well established that polyphenolic compounds have powerful antioxidant properties, through their ability to scavenge a wide range of reactive oxygen, nitrogen, and chlorine species. Antioxidant activity of polyphenols arises from their high reactivity as hydrogen or electron donors, from their capacity to chelate transition metal ions, and from the ability of polyphenolic radicals to stabilize and delocalize the unpaired electron.[28,29] In general, antioxidant activity depends on the number and positions of hydroxyl groups and other substituents on the molecule.[30] However, polyphenols can also act as pro-oxidants.[31] Under normal growth conditions phenoxyl radicals are usually rapidly changed to non-radical products by polymerization reactions or by enzymatic (as well as non-enzymatic) radical reduction. However, the pro-oxidant activity of phenolic compounds depends on their metal reducing properties, chelating behavior, and O_2-reducing ability. This latter property depends on the redox potential of the oxidized species and the lifetime of the phenoxyl radicals. Phenoxyl radicals exhibit cytotoxic pro-oxidant activity when the lifetime of the radicals is prolonged by resonance-stabilization.[18]

ROS has been shown to be an early signal for apoptosis.[32] To confirm whether radical species were involved in coumarin **8**-mediated apoptosis in U-937 cells, the production and levels of radical species were measured by ESR spectroscopy in RPMI 1640 medium in the presence or absence of cells. The experimental (A) and simulated (B) ESR spectra of the coumarin **8*** radical in RPMI 1640 cultured U-937 cells are shown in Figure 3. ESR spectrum of the coumarin **8*** radical showed a complex signal of 17 peaks, compatible with the presence of the phenoxyl radical. Similar ESR spectrum of the coumarin **8*** radical was obtained in RPMI 1640 alone (data not shown). Scheme 2 shows the resonant structures of the coumarin **8*** radical and Table 4 summarizes the hyperfine coupling constant values for the six ^1H under different experimental conditions. For the simulation of this spectrum, the hyperfine interactions of the six ^1H of the semiquinone form of the coumarin **8*** radical were considered. The simulation of the resonant structures in Scheme 2 indicates that the spectrum shown in Figure 3A is compatible with the phenoxyl radical of coumarin **8**. Given that coumarin **8** is a polyphenol, the coumarin **8** radical ($QH^{\bullet}$) may be transformed by fast deprotonation, at pH 7.6 to its more stable semiquinone form ($Q^{\bullet -}$).[33]

$$QH_2 \xrightarrow{R^{\bullet};O_2;\text{Active metals}} QH^{\bullet} \quad (1)$$

$$QH^{\bullet} \longrightarrow Q^{\bullet -} + H^{+} \quad (2)$$

This semiquinone form ($Q^{\bullet -}$) in the presence of oxygen may thus generate superoxide radicals.[31]

$$Q^{\bullet -} + O_2 \longrightarrow Q + O_2^{\bullet -} \quad (3)$$

The superoxide radicals can promote various secondary reactions leading to the generation of ROS and other radical species as shown by the following equations:

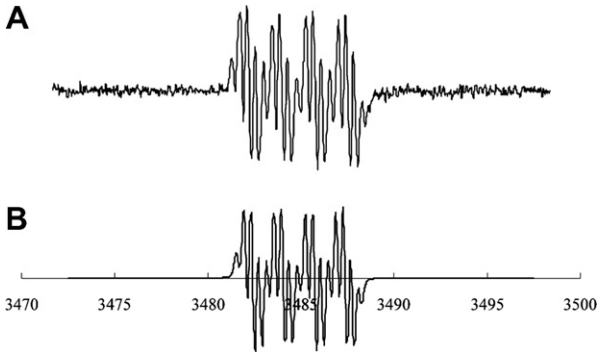

Figure 3. Experimental (A) and simulated (B) ESR spectra of the coumarin **8*** radical in RPMI 1640 in the presence of U-937 cells. Experimental ESR spectrum was recorded at 20 °C in an X-band ESR Spectrometer Bruker ECS 106. The spectrometer settings were: microwave power 10.1 mW, conversion time 2.56 ms, time constant 2.56 ms, modulation frequency 50 kHz, modulation amplitude 0.107 G, gain 2×10^4, resolution 1024 points, sweep width 25 G, number of scans 100. Simulated spectrum was obtained by the calculation of the quantum density matrix using the Liouville equation with the incorporation of the modulated Zeeman effect. The hyperfine interactions of the six ^1H of the semiquinone form of the coumarin **8*** radical were considered for the simulation of this spectrum.

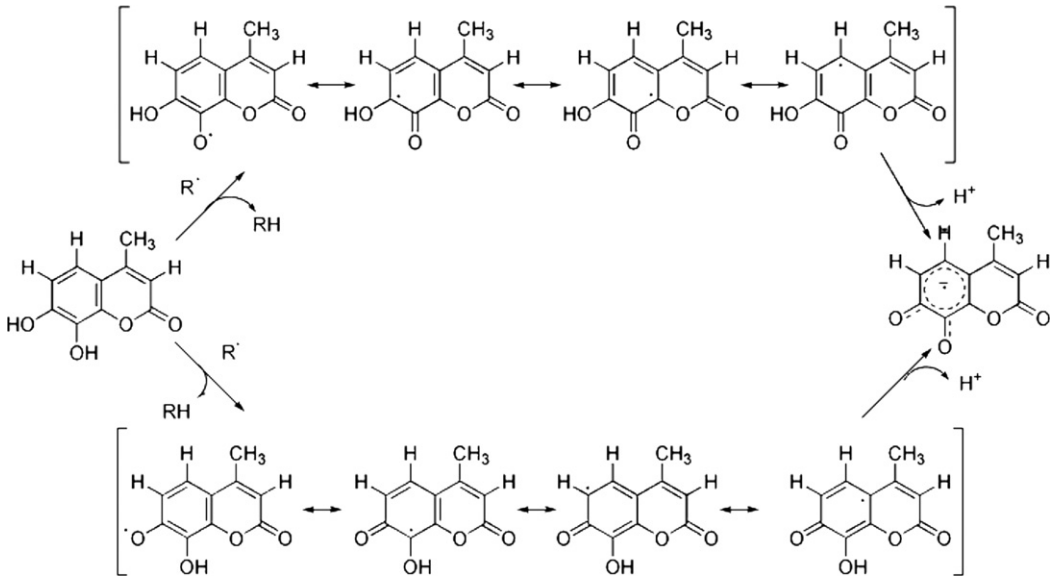

Scheme 2. Resonant structures of the phenoxyl radical of coumarin **8*** and the formation of its semiquinone form. The simulated ESR spectrum of the semiquinone form was compatible with the experimental ESR spectrum obtained when coumarin **8** was added to RPMI 1640 and to cultured U-937 cells in RPMI 1640.

Table 4. Hyperfine coupling constants ± SEM (n = 5) of the six ^{1}H of the coumarin **8*** radical semiquinone form in different mediums at pH 7.6: PBS, RPMI 1640, and U-937 cells in RPMI 1640

Medium	aH1 (G)	aH2 (G)	aCH_3(G)	aH6 (G)
PBS 100 mM	3.29 ± 0.06	1.84 ± 0.04	0.42 ± 0.02	0.31 ± 0.01
RPMI 1640	3.32 ± 0.06	1.64 ± 0.03	0.41 ± 0.02	0.30 ± 0.01
U-937 cells in RPMI 1640	3.32 ± 0.05	1.63 ± 0.03	0.42 ± 0.02	0.32 ± 0.01

$$O_2^{\cdot-} + O_2^{\cdot-} + 2H^+ \longrightarrow O_2 + H_2O_2 \quad (4)$$

$$H_2O_2 + Me^{n+}_{active} \longrightarrow HO^{\cdot} + HO^- + Me^{(n+1)+}_{active} \quad (5)$$

$$HO^{\cdot} + RH \longrightarrow H_2O + R^{\cdot} \quad (6)$$

With the aim to confirm the presence of superoxide and/or other radicals, PBN spin trap was added to cultured U-937 cells exposed to coumarin **8** (Figs. 4 and 5). PBN reacts with oxygen radicals and carbon centered radicals forming PBN adducts, that can be detected by ESR spectroscopy.

Figure 4 shows the experimental (A) and simulated (B) ESR spectra obtained from U-937 cells exposed to coumarin **8** in RPMI 1640 and incubated in the presence of the spin trap PBN. Two signals were observed, one cor-

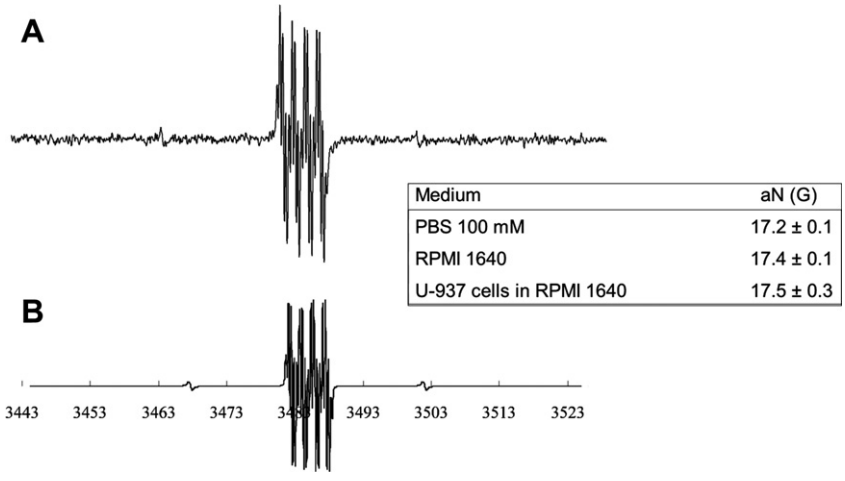

Medium	aN (G)
PBS 100 mM	17.2 ± 0.1
RPMI 1640	17.4 ± 0.1
U-937 cells in RPMI 1640	17.5 ± 0.3

Figure 4. Experimental (A) and simulated (B) ESR spectra of the coumarin **8*** radical and the PBN adduct in U-937 cells cultured in RPMI 1640. The spin trap PBN (100 mM final concentration) was added to the cell culture and both, the phenoxyl radical and the PBN-adduct, signals were simultaneously recorded in an X-band ESR Spectrometer Bruker ECS 106 at 20 °C. The spectrometer settings were same as those detailed in the legend to Figure 3 except that the sweep width was 80 G and the number of scans 400. Simulated spectrum of coumarin **8*** radical was obtained as described in the legend to Figure 3. The inset shows the hyperfine coupling constants ± SEM (n = 7) of the ^{14}N PBN adducts in different experimental conditions.

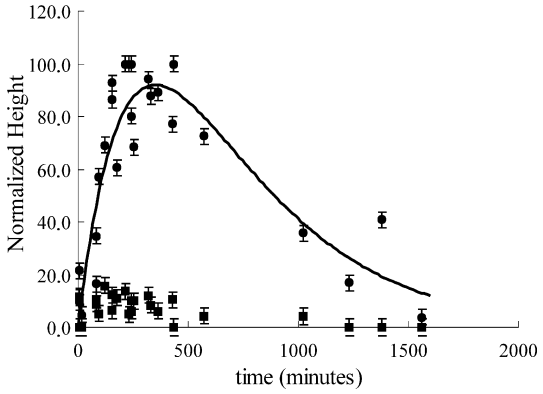

Figure 5. Kinetic of the coumarin **8*** radical (•) and the PBN adduct (■) in cultured U-937 cells. Cells growing in exponential phase (10^{6} cells/ml) were incubated with 2 mM coumarin **8** in RPMI 1640 at 37 °C in the presence of the spin trap PBN (100 mM). The ESR signals of the coumarin **8*** radical and the PBN-adduct were followed as function of time, using the spectrometer settings detailed in the legend of Figure 4. The signal intensity of the coumarin **8*** radical was measured as the total height of the third low field peak (h_{+3}) in the first derivative spectrum, whereas that of the PBN adduct was determined as the total height of the first low field peak (h_{+1}). As the ESR spectra had equivalent line-shapes and line-widths at different times, the intensity of the signal was proportional to the radical concentration. Normalized heights were calculated as the percentage relationship between the height of the ESR signal at a given time and the maximum height value of the signal obtained in the respective experience. The kinetic curve of the coumarin **8*** radical was fitted according to Eq. 1. Data correspond to five independent experiments.

responding to the described coumarin **8*** radical and the other to the PBN adduct. The ESR signal of the PBN adduct showed the three characteristic peaks of the hyperfine interaction with the ^{14}N, being the central peak superimposed with the coumarin **8*** radical signal. The inset in Figure 4 summarizes the hyperfine coupling constant values for the ^{14}N of the PBN adduct under different experimental conditions. The high hyperfine coupling constant values obtained for the ^{14}N of the PBN adduct suggest that the radical trapped with PBN was not oxygen centered.[34,35]

These findings suggest that radical species were generated from coumarin **8** in RPMI 1640 medium as well as in U-937 cells cultured in RPMI 1640. Therefore a time course study of radical species production was carried out. The kinetics for the coumarin **8*** radical and the PBN adduct in cell culture are shown in Figure 5. In order to plot the values obtained under different experimental conditions the heights of the coumarin **8*** radical ESR signal at different times were normalized to the maximum height value obtained in each experimental procedure. Using a computational program, the kinetics of the coumarin **8*** radical was simulated and fitted by non lineal regression according to the model proposed in Eq. 7.

$$\text{Coumarin } \mathbf{8} \xrightarrow{k^{\text{obs.}}_{\text{form.}}} \text{Coumarin } \mathbf{8}^{*} \text{ radical} \xrightarrow{k^{\text{obs.}}_{\text{decom.}}} \text{ESR silent products} \quad (7)$$

The higher production of phenoxyl radical and PBN adduct in U-937 cells treated with coumarin **8** appeared roughly as early as 2 h (Fig. 5). PBN adduct shows a similar kinetics profile to coumarin **8*** radical, being an indirect verification of ROS production. Figure 6 shows the kinetic of the coumarin **8*** radical in RPMI 1640 medium alone and in U-937 cells in RPMI 1640. Both kinetics were simulated and fitted as previously described. The first order rate constants, corresponding to the formation ($k^{\text{obs.}}_{\text{form.}}$) and decomposition ($k^{\text{obs.}}_{\text{decom.}}$) of the coumarin **8*** radical calculated in cultured U-937 cells in RPMI 1640 and the medium alone were: $k^{\text{obs.}}_{\text{form.}} = 1.2 \times 10^{-4}\ \text{s}^{-1}$, $k^{\text{obs.}}_{\text{decom.}} = 1.3 \times 10^{-4}\ \text{s}^{-1}$ and $k^{\text{obs.}}_{\text{form.}} = 4.5 \times 10^{-5}\ \text{s}^{-1}$ and $k^{\text{obs.}}_{\text{decom.}} = 5.0 \times 10^{-5}\ \text{s}^{-1}$, respectively. The difference between both constants, $k^{\text{obs}}_{\text{form}}$ and $k^{\text{obs}}_{\text{decom}}$, suggests a distinct kinetic behavior in the formation and decomposition of the coumarin **8*** radical in different conditions (Fig. 6). Whether this different kinetic behavior is implicated in the pro-apoptotic effect of coumarin **8** is presently unknown and requires further studies.

Kim and co-workers[17] reported that anti-oxidant treatment completely prevents scopoletin-induced apoptosis in HL-60 promyelocytic cells, suggesting that ROS generation may play an important role in the pro-apoptotic activity of this coumarin. As in the present study we observed that hydroxylated coumarins induced apoptosis in U-937 promonocytic cells, we next evaluated whether ROS generation was implicated in the pro-apoptotic activity of these coumarins. The exposure of 10 mM *N*-acetyl-L-cysteine-treated U-937 cells to coumarin **8** for 24 h resulted in the suppression of the ESR signal of the coumarin **8*** radical and PBN-adduct generation (data not shown). To further evaluate the participation of ROS in coumarin **8**-induced apoptosis, we studied

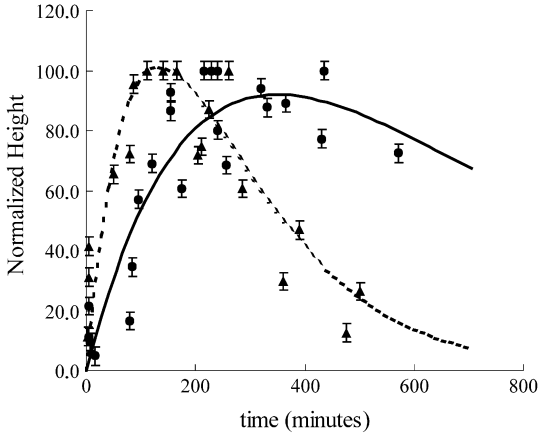

Figure 6. Coumarin **8*** radical kinetic in RPMI 1640 medium (▲, segmented line) and in U-937 cells cultured in RPMI 1640 (•, continuous line). Coumarin **8** (2 mM) was added to U-937 cells growing in exponential phase (10^{6} cells/ml) and to RPMI 1640 alone followed by incubation at 37 °C. The ESR signal of coumarin **8*** radical was followed as function of time, using the spectrometer settings detailed in the legend of Fig. 4. Signal intensities and normalized heights were obtained as described in Fig. 5. The kinetics curves were fitted according to equation Eq. 1. Data correspond to five independent experiments.

the pro-apoptotic effect of this coumarin in the presence of the radical scavenger NAC by using two different approaches. U-937 cells were exposed to 250 μM coumarin **8** for 24 h and NAC (10 mM) was added to the cell culture either every 8 h for 24 h or just once 24 h before the end of the assay. The first approach fully inhibited the appearance of a ladder-like pattern of DNA fragments and blocked coumarin **8**-triggered apoptosis in U-937 cells (Fig. 7B). However, the second treatment did not abolish DNA fragmentation in coumarin **8**-treated cells (Fig. 7A). In the two experimental treatments NAC exerted a protective role, although the effect was further evident when cells were repeatedly exposed to the radical scavenger. The underlying reasons for the difference between the two treatments remain presently unknown. Taken together, these findings support that ROS and/or other radical species play a critical role in the induction of cell death by coumarin **8**. In the presence of O_2, transition metals such as Cu^{2+} and Fe^{2+} catalyze the redox cycling of phenolics, leading to the formation of ROS and other organic radicals that can eventually damage DNA, lipids, and other biological molecules.[18] ROS may trigger mitochondrial membrane polarization, which involves drastic alterations in cell metabolism and the release of apoptogenic proteins that initiate caspase-dependent as well as caspase-independent pathways.[36,37] However, the intracellular targets of the phenoxyl radical or other generated ROS that mediate the induction of programmed cell death by coumarin **8** in U-937 cells remain to be elucidated.

In order to gain insight into the radical production of hydroxycoumarins and related compounds in U-937 cells, the generation of phenoxyl radicals was assessed by ESR spectroscopy. In the case of coumarin **8**, the phenoxyl radical was detected by ESR spectroscopy. However compounds **7** and **3** induced the formation of phenoxyl radicals but they were detected at higher concentrations and pH values than coumarin **8**. As expected, no phenoxyl radicals were produced by the remaining coumarins that did not possess a free phenolic hydroxyl group (**1**, **4**–**6**, **10**, **11**, and **13**) (data not shown). In addition, compound **2** failed to produce phenoxyl radicals detectable by ESR spectroscopy, likely as the result of its particular electronical properties. It has been previously reported that monohydroxycoumarins, such as **3**, induce apoptosis in leukemic cells through radical generation.[17] In the present study, coumarin **3** showed a weaker biological activity as compared to **8**, since monohydroxycoumarins generate less radical species. A similar behavior was observed for monohydroxycoumarins **7** and **9**. Furthermore, the replacement of the 7-OH by an amino group (coumarin **10**) suppressed both radical generation and the biological activity. In compound **12**, the presence of a $–CF_3$ group in C-4 inhibited the formation of the phenoxy radical thus resulting in the loss of biological activity. These findings support the existence of a direct relationship between the biological activity and the pro-oxidant properties of these compounds limited by the number of radical species stabilized by resonance.

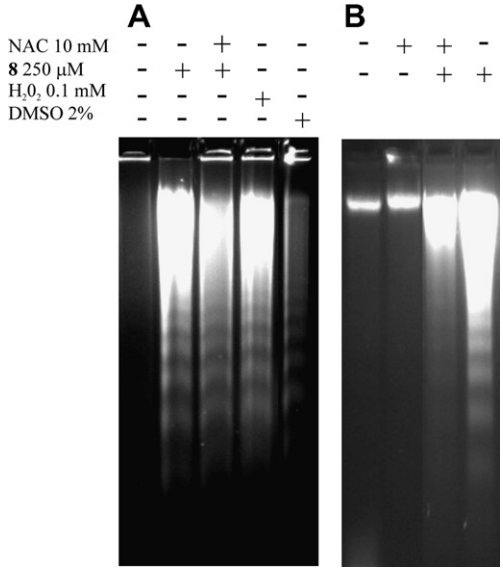

Figure 7. DNA fragmentation analysis. (A) U-937 cells were pretreated once with 10 mM NAC (pH 7.0) at 24 h before the end of the assay. Cells were also co-incubated with 0.1 mM H_2O_2 or 2% DMSO (positive control). Similar results were obtained in three independent experiments. (B) U-937 cells were exposed to 250 μM coumarin **8** and 10 mM NAC (pH 7.0) was added to the cell culture every 8 h for 24 h. NAC (10 mM) treated U-937 cells were used as negative control. Similar results were obtained in three independent experiments.

Over the last years coumarins and derivatives were extensively studied and multiple biological effects were reported for these compounds. In the present work, structurally related hydroxycoumarins were studied in order to elucidate the key structural requirements to induce apoptosis in leukemic cells. We showed that the dihydroxylated coumarin **8** induced apoptosis through ROS generation in human leukemic cells. To our knowledge, this is the first report to show that dihydroxylated coumarins at cytotoxic micromolar concentration induced apoptosis mediated by ROS in U-937 cells. We have recently demonstrated that dihydroxylated coumarins failed to induce apoptosis in normal cells as mature human monocytic[5] or human umbilical vein endothelial cells (HUVEC) (unpublished observations). The present study further suggests that dihydroxylated coumarins are likely promising therapeutic drugs for cancer treatment due to their pro-apoptotic activity in cancer cells but minimal toxicity in normal cells.

3. Materials and methods

3.1. Chemicals

RPMI medium 1640, phosphate-buffered saline (PBS), *N*-*t*-butyl-α-phenylnitrone (PBN), *N*-acetyl-L-cysteine (NAC), dimethylsulfoxide (DMSO), and commercial coumarins were obtained from Sigma Chemical Co. (St. Louis, MO, USA). Fetal calf serum was purchased from Natocor (Argentina). All commercial chemicals and solvents were of reagent grade and used without further purification unless otherwise specified.

3.2. Chemistry

Standard workup procedures were used for all chemical reactions, and solvents were dried over $MgSO_4$ before evaporation. The general procedure for coumarin synthesis was as follows: 6 ml of concentrated sulfuric acid was placed in a 100-ml flask on ice bath followed by the dropwise addition under magnetic stirring of a solution containing 10 mmol phenol in 1.4 ml (11 mmol) of ethyl acetoacetate. After one hour the reaction mixture was poured into crushed ice and the precipitate collected by suction filtration and then washed with cold water. The crude coumarin was recrystallized from 95% ethanol. Reactions were monitored by thin-layer chromatography on 0.25 mm silica gel plates (Merck Kieselgel 60*F254*) and visualized by UV light. All compounds were purified by recrystallization from ethanol and characterized by IR and nmR spectra as well as by melting point determination. ^{1}H RMN and ^{13}C RMN data were recorded on a Bruker Advance 500 spectrometer. Chemical shifts are reported in parts per million (ppm) and calibrated to the deuterated solvent reference peaks. Coupling constants are reported in units of hertz (Hz). Infrared spectra were recorded on a Perkin-Elmer Spectrum One apparatus from KBr disks (resolution: 4 cm^{-1}). Melting points were determined with a Thomas Hoover Unimelt apparatus and are uncorrected.

3.3. Compounds

3.3.1. 4,6-Dimethylcoumarin (6)
Yield: 60%.

Mp 147–149 °C (ethanol); lit.[38] 149–150 °C.

^{1}H nmR (DMSO-d_6) 2.38 (s, 3H), 2.41 (d, J = 1.3 Hz,1H), 6.37 (d, J = 1.3 Hz, 1H), 7.28 (d, J = 8.5 Hz, 1H), 7.43 (dd, J = 8.5 Hz,1.5 Hz, 1H), 7.57 (d, J = 1.3 Hz, 1H).

IR (v, cm^{-1}) 1715.8.

3.3.2. 4,7-Dimethylcoumarin (5)
Yield: 65%.

Mp 128–130 °C (ethanol); lit.[39] 131 °C (ethanol).

^{1}H nmR (DMSO-d_6) 2.40 (s, 6H), 6.30 (s, 1H), 7.19 (d, J = 8.5 Hz, 1H), 7.20 (s, 1H), 7.64 (d, J = 8.0 Hz, 1H).

IR (v, cm^{-1}) 1704.3, 1720.7.

3.3.3. 4,8-Dimethylcoumarin (4)
Yield: 20%.

Mp 111–113 °C (ethanol); lit.[38] 114 °C (ethanol).

^{1}H nmR (DMSO-d_6) 2.36 (s, 3H), 2.42 (d, J = 1.3 Hz, 3H), 6.39 (d, J = 1.0 Hz, 1H), 7.26 (t, J = 7.6, 1H), 7.50 (d, J = 6.9, 1H), 7.60 (d, J = 7.9 Hz, 1H).

IR (v, cm^{-1}) 1708.5.

3.3.4. 7-hydroxy-4-methylcoumarin (7)
Yield: 85%.

Mp 184–185 °C (ethanol); lit.[40] 185 °C.

^{1}H nmR (DMSO-d_6) 2.36 (s, 3H), 6.12 (d, 1H, J = 1.3 Hz), 6.69 (d, 1H, J = 2.63 Hz), 6.79 (dd, 1H, J = 8.5, 2.3 Hz), 7.59 (d, 1H, J = 8.5), 10.53 (s, 1H).

IR (v, cm-1) 1600.6, 1678.2, 3159.1.

3.3.5. 7,8-Dihydroxy-4-methylcoumarin (8)
Yield: 80%.

Mp 242–244 °C (ethanol); lit.[40] 243–244 °C.

^{1}H nmR (DMSO-d_6) 2.36 (s, 3H), 6.13 (d, J = 0.9 Hz, 1H), 6.82 (d, J = 8.5 Hz, 1H), 7.10 (d, J = 8.7 Hz, 1H).

IR (v, cm^{-1}) 1583.8, 1600.0, 1620.2, 1648.4, 3412.9.

3.3.6. 6-Hydroxy-4-methylcoumarin (9)
Yield: 40%.

Mp 239–241 °C (ethanol); lit.[40] 241–242 °C.

1HNMR (DMSO-d_6) 2.44 (d, J = 1.2 Hz, 3H), 6.42 (d, J = 1.2 Hz, 1H), 7.10 (s, 1H), 7.11 (dd, J = 7.0 Hz, 2.8 Hz, 1H), 7.30 (dd, J = 6.6 Hz, 2.7 Hz, 1H), 9.8 (s, 1H).

IR (v, cm-1) 1690.0, 3336.2.

All synthesized and commercial coumarins (Table 1) were dissolved in 0.01% (v/v) DMSO and stored at −20 °C.

3.4. Cell culture

The U-937 cell line (American Type Culture Collection, Rockville, MD) was cultured at 37 °C in a humidified atmosphere with 5% CO_2 in RPMI 1640 medium, supplemented with 10% fetal calf serum and 50 μg/ml gentamicin. The cell suspension was split at the third day and diluted 1 day before experimental procedures.

3.5. Measurement of the cytotoxicity concentration 50 (CC_{50})

Cells growing in exponential phase were seeded at 10^5 cells in 1 ml of RPMI 1640 in a 24-well culture plate and incubated in a 5% CO_2 atmosphere. Cells were exposed to different concentrations of coumarins (0.15 μM to 2.0 mM) or 0.0001% (v/v) DMSO (control group). After incubation for 48 h, an aliquot of each treatment was collected and mixed with an equal volume of 0.4% Trypan blue and incubated for 5 min after which the number of viable cells was estimated by a hemocytometer chamber. The cytotoxic concentration 50 (CC_{50}) values were calculated with the equation for sigmoidal dose response using Prism 4.00 for Windows (GraphPad Software, San Diego, CA). Assays were car-

ried out by triplicate in at least three independent experiments.

3.6. Cell growth inhibition assays (IC_{50})

Cells growing in exponential phase were seeded at 10^4 cells in 150 μl of RPMI 1640 in a 96-well culture plate and incubated under a 5% CO_2 atmosphere. U-937 cells were exposed to different concentrations of coumarins ranging from 0.15 μM to 2.0 mM or to 0.0001% (v/v) DMSO (control group) followed by incubation with 0.5 μCi of [^{3}H]Methyl-thymidine (Perkin-Elmer, USA), added 12 h before the end of the experiment and then harvested in an automatic cell harvester (Nunc, Maryland, USA). The incorporation of the radioactive nucleotide was measured in a Pharmacia Wallac 1410 liquid scintillation counter and expressed as incorporation percentage with respect to the control group (cells treated with DMSO). The inhibitory proliferation concentration 50 (IC_{50}) values were calculated using the equation for sigmoidal dose response using Prism 4.00 for Windows (GraphPad Software, San Diego, CA). Assays were performed by quadruplicate in at least four independent experiments.

3.7. Detection of DNA fragmentation by gel electrophoresis

DNA from untreated or coumarin-treated U-937 cells was analyzed for endonucleolytic DNA damage, using horizontal agarose gel electrophoresis. Cells were incubated for 24 h in the presence of coumarins or pretreated with 10 mM *N*-acetyl-L-cysteine (pH 7.0). Cell aliquots (3.10^6 cells) were collected, washed with PBS, and lysed in a buffer containing 100 mM NaCl, 4 mM EDTA, 50 mM Tris–HCl, 0.5% SDS, pH 8.0, and proteinase K (100 mg/ml) at 55 °C for 2 h. DNA was then extracted and purified as described by Parborell et al.[41] Electrophoresis was performed for 2.30 h at 40 V in 1.8% agarose gels containing ethidium bromide at a final concentration of 0.1 mg/ml in TBE buffer (89 mM Tris, 89 mM boric acid, 2 mM EDTA at pH 8.0). DNA banding was visualized with an UV transilluminator.

3.8. Evaluation of cellular morphological changes

Cells growing in exponential phase were seeded at 10^5 cells in 2 ml of RPMI 1640 in a 24-well culture plate and incubated under a 5% CO_2 atmosphere. Cells were exposed to 0.15 μM to 2.5 mM coumarins or 0.0001% (v/v) DMSO (control group) and the cellular morphology examined after incubation for 24 or 48 h. Cells (10^5) were suspended in 100 μl PBS containing 2 μg/ml Hoechst 33342 nuclear dye (HO, Sigma, St. Louis, USA) and 12 μg/ml propidium iodide (PI; Sigma, St. Louis, USA). After incubation at 37 °C for 8 min, cells were observed under a fluorescence microscope (Zeiss, Germany) under UV light at 430 nm (HO) and 630 nm (PI). Apoptotic cells show a high Hoechst 33342 (HO) staining but a low propidium iodide (PI) staining, since they initially tend to exclude PI. Necrotic cells are brightly stained with PI, whereas healthy cells are dimly stained by HO and unstained by PI.[24] The number of apoptotic cells was estimated by using a hemocytometer chamber. Ten randomly selected fields were acquired from each treatment and one hundred cells were minimally counted. Assays were carried out by triplicate in at least three independent experiments.

In addition, cytospin preparations of cell suspensions were fixed and stained with May Grunwald–Giemsa and cell morphology determined by light microscopy (Zeiss, Germany).

3.9. Electron spin resonance (ESR) experiments

U-937 cells growing in exponential phase (10^6 cells/ml) were incubated with 2 mM coumarin **8** in RPMI at 37 °C. The electron spin resonance (ESR) signal of the phenoxyl radical of coumarin **8** was registered along time. In another experiment the spin trap *N*-*t*-butyl-α-phenylnitrone (PBN) (100 mM) was added to the medium and both, the phenoxyl radical and the PBN-adduct, signals were detected with time. In both experiments, aliquots from the media were drawn at different periods of time (0–24 h) and the ESR spectra recorded at 20 °C in an X-band ESR Spectrometer Bruker ECS 106 (Brucker Instruments Inc., Berlin, Germany). The spectrometer settings were: microwave power 10.1 mW, conversion time 2.56 ms, time constant 2.56 ms, modulation frequency 50 kHz, modulation amplitude 0.107 G, gain 2×10^4, resolution 1024 points. Spectra were obtained using a sweep width of 25 G for the characterization of coumarin **8*** radical signals and a sweep width of 80 G for the detection of both, coumarin **8*** radical and PBN-adduct, signals simultaneously. The number of scans varied from 100 to 400 depending on the signal intensity.

The signal intensity of the coumarin **8*** radical was measured as the total height of the third low field peak (h_{+3}) in the first derivative spectrum whereas that of the PBN adduct was determined as the total height of the first low field peak (h_{+1}). As the ESR spectra had equivalent lineshapes and line-widths at different times, the intensity of the signal was proportional to the radical concentration. The coumarin **8*** radical concentration and the PBN adduct yields were estimated from the total heights of their respective peaks. The adduct yield corresponds to the amount accumulated in a fixed period of time. Simulated spectra were obtained by calculating the quantum density matrix using the Liouville equation with the incorporation of the modulated Zeeman effect.[42] The kinetics were simulated by numeric resolution of the differential equations using the fifth order Kutta–Merson algorithm.[43,44] No linear regression fits were performed using a modification of the Levenberg Marquart algorithm.[45]

Acknowledgments

We are sincerely grateful to Dr. L. Bianciotti for critical reading of the manuscript. This study was supported by grants from the Universidad de Buenos Aires (Grant UBACyT B0-50); Consejo Nacional de Investigaciones Científicas y Técnicas (PIP 6110), SECYT (PICT-05-12164), and Fundación Bunge Born fellowship 'Jorge Oster' 2004 to the first author.

References and notes

1. Leszczyniecka, M.; Roberts, T.; Dent, P.; Grant, S.; Fisher, P. B. *Pharmacol. Ther.* **2001**, *90*, 105–156.
2. Kaufmann, S. H. *Cancer Res.* **1989**, *49*, 5870–5878.
3. Meng, X. W.; Lee, S. H.; Kaufmann, S. H. *Curr. Opin. Cell Biol.* **2006**, *18*, 668–676.
4. Eugenia Riveiro, M.; Shayo, C.; Monczor, F.; Fernandez, N.; Baldi, A.; De Kimpe, N.; Rossi, J.; Debenedetti, S.; Davio, C. *Cancer Lett.* **2004**, *210*, 179–188.
5. Riveiro, M. E.; Vazquez, R.; Moglioni, A.; Gomez, N.; Baldi, A.; Davio, C.; Shayo, C. *Biochem Pharmacol*. 2007, doi:10.1016/j.bcp.2007.09.025.
6. Borges, F.; Roleira, F.; Milhazes, N.; Santana, L.; Uriarte, E. *Curr. Med. Chem.* **2005**, *12*, 887–916.
7. Curini, M.; Cravotto, G.; Epifano, F.; Giannone, G. *Curr. Med. Chem.* **2006**, *13*, 199–222.
8. Hoult, J. R.; Paya, M. *Gen. Pharmacol.* **1996**, *27*, 713–722.
9. Manolov, I.; Topashka-Ancheva, M.; Klouchek, E. *Eksp. Med. Morfol.* **1993**, *31*, 49–60.
10. Fylaktakidou, K. C.; Hadjipavlou-Litina, D. J.; Litinas, K. E.; Nicolaides, D. N. *Curr. Pharm. Des.* **2004**, *10*, 3813–3833.
11. Kostova, I.; Raleva, S.; Genova, P.; Argirova, R. *Bioinor. Chem. Appl.* **2005**, *2006*, 1–9.
12. Kawase, M.; Sakagami, H.; Motohashi, N.; Hauer, H.; Chatterjee, S. S.; Spengler, G.; Vigyikanne, A. V.; Molnar, A.; Molnar, J. *In Vivo* **2005**, *19*, 705–711.
13. Egan, D.; O'Kennedy, R.; Moran, E.; Cox, D.; Prosser, E.; Thornes, R. D. *Drug Metab. Rev.* **1990**, *22*, 503–529.
14. Finn, G.; Creaven, B.; Egan, D. *Eur. J. Pharmacol.* **2003**, *481*, 159–167.
15. Kolodziej, H.; Kayser, O.; Woerdenbag, H. J.; van Uden, W.; Pras, N. *Z. Naturforsch., C* **1997**, *52*, 240–244.
16. Chu, C. Y.; Tsai, Y. Y.; Wang, C. J.; Lin, W. L.; Tseng, T. H. *Eur. J. Pharmacol.* **2001**, *416*, 25–32.
17. Kim, E. K.; Kwon, K. B.; Shin, B. C.; Seo, E. A.; Lee, Y. R.; Kim, J. S.; Park, J. W.; Park, B. H.; Ryu, D. G. *Life Sci.* **2005**, *77*, 824–836.
18. Sakihama, Y.; Cohen, M. F.; Grace, S. C.; Yamasaki, H. *Toxicology* **2002**, *177*, 67–80.
19. Whang, W. K.; Park, H. S.; Ham, I.; Oh, M.; Namkoong, H.; Kim, H. K.; Hwang, D. W.; Hur, S. Y.; Kim, T. E.; Park, Y. G.; Kim, J. R.; Kim, J. W. *Exp. Mol. Med.* **2005**, *37*, 436–446.
20. Sharma, S. D.; Rajor, H. K.; Chopra, S.; Sharma, R. K. *Biometals* **2005**, *18*, 143–154.
21. Decker, E. A. *Nutr. Rev.* **1997**, *55*, 396–398.
22. Hadi, S. M.; Asad, S. F.; Singh, S.; Ahmad, A. *IUBMB Life* **2000**, *50*, 167–171.
23. Wyllie, A. H.; Kerr, J. F.; Currie, A. R. *Int. Rev. Cytol.* **1980**, *68*, 251–306.
24. Zauli, G.; Vitale, M.; Re, M. C.; Furlini, G.; Zamai, L.; Falcieri, E.; Gibellini, D.; Visani, G.; Davis, B. R.; Capitani, S., et al. *Blood* **1994**, *83*, 167–175.
25. Martinsson, P.; Liminga, G.; Nygren, P.; Larsson, R. *Anticancer Drugs* **2001**, *12*, 699–705.
26. Ma, J.; Jones, S. H.; Hecht, S. M. *J. Nat. Prod.* **2004**, *67*, 1614–1616.
27. Kimura, Y.; Okuda, H.; Arichi, S.; Baba, K.; Kozawa, M. *Biochim. Biophys. Acta* **1985**, *834*, 224–229.
28. Blokhina, O.; Virolainen, E.; Fagerstedt, K. V. *Ann. Bot. (Lond.)* **2003**, *91 Spec. No*, 179–194.
29. Rice-Evans, C. A.; Sampson, J.; Bramley, P. M.; Holloway, D. E. *Free Radic. Res.* **1997**, *26*, 381–398.
30. Cai, Y. Z.; Mei, S.; Jie, X.; Luo, Q.; Corke, H. *Life Sci.* **2006**, *78*, 2872–2888.
31. Roginsky, V.; Barsukova, T.; Loshadkin, D.; Pliss, E. *Chem. Phys. Lipids* **2003**, *125*, 49–58.
32. Simon, H. U.; Haj-Yehia, A.; Levi-Schaffer, F. *Apoptosis* **2000**, *5*, 415–418.
33. Roginsky, V.; Lissi, E. *Food Chem.* **2005**, *92*, 235–254.
34. Buettner, G. R. *Free Radic. Biol. Med.* **1987**, *3*, 259–303.
35. Available from: http://EPR.niehs.nih.gov. In NIEHS/NIH, 2004.
36. Kroemer, G. *Biochem. Biophys. Res. Commun.* **2003**, *304*, 433–435.
37. Mates, J. M.; Sanchez-Jimenez, F. M. *Int. J. Biochem. Cell Biol.* **2000**, *32*, 157–170.
38. Chakravarti, D.; Dutta, N. *J. Indian Chem. Soc.* **1940**, *17*, 65–71.
39. Osborne, A. G. *Tetrahedron* **1981**, *37*, 2021–2025.
40. Rajithaa, B.; Kumara, V. N.; Someshwara, P.; Madhava, J. V.; Reddy, P. N.; Reddyb, Y. H. *General Papers ARKIVOC* **2006**, *12*, 23–27.
41. Parborell, F.; Irusta, G.; Vitale, A.; Gonzalez, O.; Pecci, A.; Tesone, M. *Biol. Reprod.* **2005**, *72*, 659–666.
42. Kalin, M.; Gromov, I.; Schweiger, A. *J. Magn. Reson.* **2003**, *160*, 166–182.
43. Golub, G. H.; Ortega, J. M. *Scientific Computing and Differential Equations: An Introduction to Numerical Methods*; Academic Press: New York, 1992.
44. Press, W.H.; Teukolsky, S.A.; Verrling, W.T.; Flannery, B.P. Numerical Recipes in Fortran: The Art of Scientific Computing. Cambridge. UK, 1992.
45. Budil, D. E.; Lee, S.; Saxena, S.; Freed, J. H. *J. Magn. Reson. A* **1996**, *120*, 155–189.